Lawrence Berkeley National Laboratory
Recent Work

Title
THE OCCURRENCE OF THE H-+ ION IN THE MASS SPECTRA OF ORGANIC COMPOUNDS

Permalink
https://escholarship.org/uc/item/6cf542bd

Authors
Newton, Amos S.
Sciamanna, A.F.
Thomas, G.E.

Publication Date
1970-06-01

eScholarship.org Powered by the California Digital Library
University of California

Submitted to International Journal of
Mass Spectrometry and Ion Physics

UCRL-19916 Rev.
Preprint

C. 2

THE OCCURRENCE OF THE H_3^+ ION IN THE MASS SPECTRA OF ORGANIC COMPOUNDS

Amos S. Newton, A. F. Sciamanna, and G. E. Thomas

September 1970

AEC Contract No. W-7405-eng-48

TWO-WEEK LOAN COPY

This is a Library Circulating Copy which may be borrowed for two weeks. For a personal retention copy, call Tech. Info. Division, Ext. 5545

LAWRENCE RADIATION LABORATORY
UNIVERSITY of CALIFORNIA BERKELEY

UCRL-19916 Rev.
C. 2

DISCLAIMER

This document was prepared as an account of work sponsored by the United States Government. While this document is believed to contain correct information, neither the United States Government nor any agency thereof, nor the Regents of the University of California, nor any of their employees, makes any warranty, express or implied, or assumes any legal responsibility for the accuracy, completeness, or usefulness of any information, apparatus, product, or process disclosed, or represents that its use would not infringe privately owned rights. Reference herein to any specific commercial product, process, or service by its trade name, trademark, manufacturer, or otherwise, does not necessarily constitute or imply its endorsement, recommendation, or favoring by the United States Government or any agency thereof, or the Regents of the University of California. The views and opinions of authors expressed herein do not necessarily state or reflect those of the United States Government or any agency thereof or the Regents of the University of California.

THE OCCURRENCE OF THE H_3^+ ION IN THE MASS SPECTRA OF ORGANIC COMPOUNDS

Amos S. Newton, A. F. Sciamanna, and G. E. Thomas

Lawrence Radiation Laboratory
University of California
Berkeley, California 94720

September 1970

ABSTRACT

The H_3^+ ion is shown to be a normal component of low yield in the fragmentation pattern of organic compounds (except C_2H_2). The pattern of H_3^+ is tabulated for the 70 eV mass spectrum of each of 33 compounds of various types. Specific studies of the energetics of formation of H_3^+ from CH_4, C_2H_6 and CH_3Cl, and of D_3^+ from CD_4 were conducted. The H_3^+ ion is shown to be derived from two sources, a low initial kinetic energy component which arises from fragmentation of the singly charged molecular ion and a high initial kinetic energy component whose AP and kinetic energy release is consistent with fragmentation of the doubly charged molecular ion. Systematic variations of H_3^+ pattern factors with carbon number are shown for the n-alkanes and 1-alkenes and with halogen type for the series of methyl halides.

I. INTRODUCTION

No investigation of the occurrence of H_3^+ ions in the mass spectra of organic compounds has been made except for an early study by Smith[1]. In his investigation Smith showed that H_3^+ ions occurred in the mass spectrum of methane, the intensity of the H_3^+ peak was linear with pressure, and the appearance potential, AP, of H_3^+ was reported to be 25.3±1 eV, about two electron volts lower than the AP of H_2^+ from methane.

In the present investigation the occurrence of H_3^+ in the mass spectrum of methane has been restudied and the study extended to other organic compounds. In the present limited survey, no organic compound other than acetylene failed to exhibit a mass peak due to the occurrence of H_3^+.

II. EXPERIMENTAL

The present work was done with a Consolidated Electrodynamics Corp. Model 21-103B mass spectrometer. Modifications to increase the sensitivity of the recording system, the vacuum capabilities of the instrument, and modifications to record directly ionization efficiency curves on an X-Y recorder have been described previously[2,3]. In the present investigation negative-repeller studies were performed by use of batteries in the modified repeller circuit. Under these conditions peaks were scanned by a motor drive of the magnet current control. Repeller potentials were measured with a battery operated vacuum tube voltmeter which was at the potential of the ion source. Metastable suppressor cutoff curves were determined with a multiple decade potential divider. In the first three decades the resistors were trimmed to an accuracy of 0.01%. The fourth stage, a ten turn potentiometer, had a linearity of

0.1%. In all work reported here, an ionizing electron current of 38 μA was used. For AP determinations, owing to the low intensity of these peaks, equal repeller potentials of ~ 0.01 V_A were used. Under these conditions secondary effects in the ion source, e.g., space charge effects and charge exchange from ions produced at the anode, are not observed. The electron energy scale was corrected by comparison with a standard (usually He) introduced into the gas mixture so the intensity of the respective peaks at about 50 eV were approximately equal. At high metastable suppressor voltages (near cutoff) the peaks become so narrow the X-Y recording procedure could not be used owing to the possibility of drifting off the peak while scanning the electron energy scale. The ionization efficiency curves of these peaks were determined on a point to point basis, scanning the peak magnetically at each predetermined electron energy.

The hydrocarbons used were Phillips Research Grade hydrocarbons. The alkyl halides were ACS Reagent Grade chemicals. The methane used was > 99.99% pure and was obtained from Pacific Oxygen Co. The CD_4 was obtained from the Merck Sharp and Dohme Co. The CH_3F used was synthesized and purified by gas chromatography.

III. RESULTS AND DISCUSSION

In Fig. 1 is shown the linearity with inlet system pressure of H_3^+ from CH_4, D_3^+ from CD_4 and H_3^+ from C_2H_6. The peaks due to CH_4^+ and H_2^+ from CH_4 are also shown. All are linear with pressure, hence the formation of H_3^+ is assumed to occur by a unimolecular process. As a further check on this point, the ratio of M/q = 5 to M/q = 6 in CD_4 (D_2H^+/D_3^+) was measured and found to be 0.020±0.001. This corresponds to an H atom impurity of ~0.7% in the CD_4. An equimolal

mixture of CH_4 and CD_4 showed the same ratio (0.020±0.001) of M/q = 5 to M/q = 6, confirming that all three atoms in D_3^+ arise from one molecule of CD_4. These experiments confirm the earlier conclusion of Smith[1] in regard to the unimolecular character of H_3^+ production from methane.

In Table 1 are shown the yields of H_3^+ ions at a nominal ionizing voltage of 70 V from a variety of organic molecules. The measurements were made by scanning M/q = 2 at an ion accelerating voltage, V_A, of 3000 V and M/q = 3 at a voltage of 2000 volts. Since each of these ions is formed with components possessing high initial kinetic energy (vide infra) the intensity ratio of H_3^+/H_2^+ found for each compound applies only to measurements made under essentially identical conditions and should not be used on an absolute basis. They are useful in indicating trends and order of magnitude expectations of H_3^+ yields. Since our own files of mass spectral data on these compounds were obtained under conditions in which M/q = 2 was scanned at 3000 V, these data have been used to relate H_3^+ to the total ion yield of these compounds. (If the A.P.I. Mass Spectral Data[4] are used for this purpose, the H_2^+ yields will, in general, be found to be lower than those used in the present calculations owing to differences in instrument operating procedures).

For the data in Table 1, each of the compounds was studied at three pressures, usually 25, 50, and 100 μm inlet pressure. In all cases the peak sensitivity of H_3^+ and the intensity ratio of H_3^+ to H_2^+ were independent of pressure.

The only organic compound investigated in which no H_3^+ was found was C_2H_2 (not listed in Table 1) from which the formation of H_3^+ by a unimolecular process is impossible. The ratio of M/q = 3 to M/q = 2 found from C_2H_2 was

0.00030±0.00005. If all the M/q = 3 peak is due to HD, this corresponds to a deuterium content [D/(H + D)] of 0.015%. This is equal to the natural abundance of deuterium from various sources within the experimental error[5]. No H_3^+ was observed in the mass spectrum of H_2O nor was any D_3^+ observed in the mass spectrum of D_2O. The yield of D_3^+ in the mass spectrum of ND_3 was about 30% of the yield from an identical pressure of CD_4. Because of the low intensity, ND_3 was not investigated further.

The compounds CH_4, CD_4, C_2H_6, and CH_3Cl were selected for more detailed study since these compounds are relatively simple and considerable information is available on the energetics of these compounds. Fig. 2 shows voltage discrimination curves of H_3^+ from CH_4 and C_2H_6 and of D_3^+ from CD_4. The extreme slope of these curves is indicative of ions with high initial kinetic energy[6]. One may also infer from these curves that H_3^+ from CH_4 has less initial kinetic energy than does H_3^+ from C_2H_6. The slope of D_3^+ from CD_4 is also less than that of H_3^+ from CH_4 indicating slightly less initial kinetic energy for D_3^+. These curves are not sensitive functions of the initial kinetic energy, but calculations of discrimination due to initial kinetic energy by the method of Berry[6] show that the H_3^+ from CH_4 curve can be approximated with an initial kinetic energy of H_3^+ equal to 0.5 eV, that of D_3^+ from CD_4 with an initial kinetic energy of D_3^+ equal to about 0.35 eV, and that of H_3^+ from C_2H_6 with an initial kinetic energy of between 5 and 6 eV.

Other methods of evaluating initial kinetic energy are the deflection method [6,7], measurement of satellite peaks at low ion accelerating voltages[8], peak cutoff curves with an ion-retarding plate at the ion collector[9], negative-repeller cutoff curves of the ion peak[10], and peak cutoff curves measured by

retarding the ions on one of the ion accelerating slits of the ion source[11]. This last method is the most sensitive for ions with low initial kinetic energy. The equipment used could not, however, be adapted for application of this method.

In the present investigation the methods used were; 1) the measurement of satellite peaks at low ion accelerating voltage, 2) the measurement of the negative repeller cutoff, and 3) the method of retarding ions at the collector.

The measurement of satellite peaks was found to be of limited utility because of low intensity at low ion accelerating voltages (see Fig. 2) and the lack of resolution of any satellite peaks at H_3^+ in the mass spectrum of CH_4 or D_3^+ in the mass spectrum of CD_4. Satellite peaks were observed at M/q = 3 from C_2H_6 and CH_3Cl, and these gave values of the initial kinetic energy of the respective high KE components comparable to the values found by the other methods.

In the negative repeller cutoff method, the difference in the repeller cutoff voltage of an ion formed with thermal initial kinetic energy distribution and one formed with higher initial kinetic energy is equal to twice the initial kinetic energy. This results from the location of the ionizing electron beam being approximately midway between the repellers and the ion-source exit slit. Because of this placement, the ionizing electron energy is determined by the potential applied between the filament and the ion source plus approximately one-half the repeller potential. Owing to the uncertainty in this factor, the negative repeller cutoff method is not reliable at low ionizing voltages since the applied ionizing voltage must be corrected each time the repeller potential is changed. At higher ionizing voltages, where the ionization-efficiency curve

is relatively flat, this uncertainty is not a critical factor in the measurements.

In the method of retarding ions at the collector, the metastable suppressor was used as a retarding grid. The maximum potential applied to the metastable suppressor must be sufficient to retard those ions of highest initial kinetic energy. Since the metastable suppressor is an einzel lens system, it has both a focussing action (the apparent collector slitwidth narrows as the potential on the metastable suppressor is increased) and a potential well of depth such that the potential actually applied to the ions is a factor of 0.973 times the potential applied to the plates. This factor was determined by Kandel[9] for the metastable suppressor in the CEC instrument, and the measurements reported here are in agreement with this factor.

If the maximum potential applied to the metastable suppressor is defined as 1.0000 V_{mss} and the fraction of this potential required to completely retard the ions is defined as f_{mss}, then from the retarding curves of an ion formed with thermal initial kinetic energy and one formed with higher initial kinetic energy, the difference in initial kinetic energy of the two ions is given by equation (1).

$$K.E. = 0.973\, V_{mss}\, (\Delta f_{mss}) \qquad (1)$$

In this equation, Δf_{mss} is the difference between the cutoff fraction of a high initial kinetic energy ion and one whose initial kinetic energy is thermal. In measuring these cutoff curves, the ion accelerating voltage, the ionizing voltage, the repeller potential and the gas mixture were all kept constant over the duration of both determinations. The peaks were scanned by sweeping with the magnetic field. The method is most sensitive at low ion accelerating voltages

but for reasons of intensity, its use at low voltage is difficult. The present experiments were made at V_A = 2000 V and V_{mss} = 2097 V. Under these conditions both D_3^+ from CD_4 and H_3^+ from C_2H_6 and CH_3Cl could be studied under identical conditions. In order to compare curves on the same basis, the peak intensities at various values of f_{mss} were normalized with respect to the peak intensity at 0.960 V_{mss} which was set equal to 100. The accuracy of determining Δf_{mss} is about ±0.00005 for ions of reasonable intensity. With V_{mss} = 2097 V the probable error in measurement of the initial kinetic energy is ±0.1 eV.

The methods have been checked by measurement of the initial kinetic energy of the M/q = 15 satellite peak in the mass spectrum of propane. Olmsted, Street, and Newton[8], using the satellite method and a 0.75 mm collector slit-width, found this peak to be formed with 2.65 eV of initial kinetic energy. Newton and Sciamanna[14] using a 0.025 mm collector slitwidth with the satellite method found 2.85±0.05 eV. R. Fuchs[12] with an absolute calibration of the deflection method found 2.71±0.05 eV. Earlier values from 2.2 to 2.9 eV are summarized by Fuchs and Taubert[13] who assumed an average value of 2.50 eV for the initial calibration of the deflection method. The methods used in this investigation give values of 2.75±0.1 eV by the metastable suppressor cutoff method and 2.9±0.1 eV by the negative repeller method. It was concluded that these methods yield results consistent with other measurements.

Fig. 3 shows the negative repeller cutoff curves of H_3^+ and D_3^+ from CH_4 and CD_4 respectively at an ionizing electron energy of 70 eV. They show both H_3^+ and D_3^+ to have a large contribution (>90%) of low initial kinetic energy ions with each having small (<10%) component of high kinetic energy ions. It is difficult to analyze these curves to obtain initial kinetic energies of

the low energy component but the shapes suggest values of ~ 0.7 eV for H_3^+ from CH_4 and ~ 0.5 eV for D_3^+ from CD_4. The high initial kinetic energy components showed energies of 4.9 and 3.9 eV respectively.

Fig. 4 shows the metastable suppressor cutoff curves of D_3^+ from CD_4 compared to $^{22}Ne^+$ as a thermal ion standard (a small CD_5^+ contribution to M/q = 22 was separated). At a corrected electron energy of 81 eV these curves show the D_3^+ to have a small (~ 10%) component of ions of initial kinetic energy 4.0±0.1 eV and a large component of ions near thermal ($\leq$ 0.1 eV). There is no evidence of any significant contribution of ions of intermediate initial kinetic energy. A small contribution of such ions would not be detectable.

Fig. 5 shows the negative repeller cutoff curves of H_3^+ from C_2H_6 and CH_3Cl respectively at an ionizing electron energy of 90 eV. The cutoff curves of the parent ions of each are shown as standards for thermal ions. Both curves show large contributions of components with high initial kinetic energy and no indication of any appreciable contribution from ions of lower initial kinetic energy. Initial kinetic energies of 4.3±0.2 and 4.1±0.2 for H_3^+ from C_2H_6 and CH_3Cl respectively were derived from these curves.

Figs. 6 and 7 show the metastable suppressor cutoff curves of H_3^+ from C_2H_6 and CH_3Cl respectively. The cutoff of He^+ ions is used as a thermal ion standard in each case. The cutoff curves of H_3^+ (and He^+) were determined at corrected ionizing electron energies of about 83 eV and at about 7 eV above the appearance potential. At electron energies of 83 eV, each shows only a high kinetic energy component but a few volts above the appearance potential, each shows the major component to be near thermal ($\leq$ 0.2 eV) with a small contribution of a high initial kinetic energy component. Curves (not shown) determined at

electron energies a few volts higher (~ 37 eV) show a rapid increase with increase in ionizing voltage of the high kinetic energy component and no indication of any intermediate energy components. The high initial kinetic energy component of H_3^+ from C_2H_6 shows an energy of 3.8±0.1 eV and that from CH_3Cl an energy of 3.7±0.1 eV.

Ionization efficiency curves for formation of H_3^+ from CH_4 and D_3^+ from CD_4 are shown in Fig. 8. The overall shape of the curves for H_3^+ from the other compounds investigated in detail are similar, each showing a fairly weak onset followed by a strong rise to a broad plateau. The use of the metastable suppressor makes possible the separation of those H_3^+ ions possessing high initial kinetic energy compared to those from the mixed species. Fig. 9 shows the separate ionization efficiency curves of D_3^+ from CD_4 at $f_{mss} = 0.97$ where both high and low initial kinetic energy species are collected, showing an AP of 25.5 eV, and the curve at $f_{mss} = 0.98535$ where only the high initial kinetic energy ions reach the collector. Points on the latter curve show considerable scatter because of the poor signal to noise ratio with this low intensity peak. Several determinations of this curve, using both an extrapolated initial appearance and a square root extrapolation, yield a value of 35.5±2 eV for the appearance potential of the D_3^+ ions of high initial kinetic energy from CD_4.

Figs. 10 and 11 show the ionization efficiency curves for the high and the combined high and low initial kinetic energy H_3^+ ions from C_2H_6 and CH_3Cl respectively. In each case a square root extrapolation is included with the curve of the high kinetic energy component. While the combined AP curve shows a small contribution due to HD^+ below the AP of H_3^+ in each case, no such

contribution is seen in the high KE curves and points below the AP's (shown by the arrows) are zero within the limits of detectability.

In Table 2 the appearance potentials of H_3^+ for several compounds are shown together with data obtained for the high initial kinetic energy of the H_3^+ fragment. In those cases where the ratio of intensities of H_3^+ to H_2^+ is low, the HD^+ contribution at M/q = 3 interferes with the determination of the onset of the initial rise of the H_3^+ peak from fragmentation of the compound. The uncertainty in the AP is necessarily larger in these cases. In all cases except D_3^+ from CD_4, the onset of He^+ ions from an He internal standard was used to calibrate the voltage scale. In the case of CD_4, $^{22}Ne^+$ was used as a standard. The peak due to Ne^+ at M/q = 22 was separated from the small CD_5^+ peak at the same nominal mass when a 0.5 mm collector slit was used. The D_3^+ peak was also separated from the C^{+2} peak, though in any case this would not interfere with the appearance potential determination of D_3^+ since C^{+2} has a much higher AP. The AP's of H_3^+ from CH_4 and of D_3^+ from CD_4 are equal within experimental error and agree with the value of 25.3±1 eV reported by Smith[1].

In Table 1 the yields of H_3^+ and H_2^+ appear to be unrelated. This is expected since it is highly improbable that H_2^+ and H_3^+ would arise from the same set of excited states of the molecule ion, or if they did, that the relative dissociation probabilities leading to these two products would be constant from one compound to another. In Fig. 12 the yields of H_2^+ and H_3^+ from a series of normal hydrocarbons are plotted. The H_2^+ yield from n-alkanes decreases slowly with increase in carbon number from C_1 to C_8. The H_3^+ yield increases sharply from methane to ethane and then falls off rapidly with

increasing carbon number. In the series of 1-alkenes, the yield of H_3^+ from ethylene is similar in magnitude to that from methane but the yield from propylene and higher alkenes does not differ significantly from the yield from n-alkanes of the same carbon number. The data in Table 1 also indicates a small effect of structure. The yield of H_3^+ from the alkanes decreases as the alkanes become more branched. The butenes show a maximum yield from the 2-butenes, and a lesser yield when the double bond is at a terminal carbon in 1-butene or isobutene. The effects are small however, and data from many more compounds would be necessary to evaluate detailed structural effects.

Fig. 13 shows the yield of H_3^+ from each compound in the series of methyl halides. Methane is included for comparison. The yield of H_2^+ decreases slowly in this series. The H_3^+ yield from CF_4 is similar in magnitude to that from CH_4, while CH_3Cl shows a marked increase in H_3^+ yield over that observed in CH_3F. The yield from CH_3Br is a factor of 2 below that of CH_3Cl and the yield from CH_3I is a factor of 17 below that of CH_3Br. While the H_3^+ yield in this series shows no relation to the H_2^+ yield, the yields of H_2X^+ ions (also shown in Fig. 13) show a variance similar to that observed for H_3^+ ions. The yields of H_2X^+ ions were calculated from measurements made at M/q = 21 for H_2F^+ from CH_3F, at M/q = 39 for H_2Cl^+ from CH_3Cl (corrected for the abundance of ^{37}Cl), at M/q = 83 for H_2Br^+ from CH_3Br (corrected for the abundance of ^{81}Br), and at M/q = 129 for H_2I^+ from CH_3I. These peaks were each linear with pressure from 25 to 100 μm inlet pressure. The descrimination due to initial kinetic energy will be much less for H_2X^+ than for H_3^+ since the heavier H_2X^+ fragments will carry less of any initial kinetic energy released in the production of these ions than is the case for the lighter H_3^+ fragment. Therefore the yields of H_2X^+ more nearly represent absolute yields relative to the total ionization than do the yields of H_3^+.

From the data given, it is concluded that there are two mechanisms for producing H_3^+ ions from organic compounds. One leads to an ion of low initial kinetic energy and the other to an ion of high initial kinetic energy. The latter has an AP some 6 to 10 eV higher than the former. It is assumed that the low kinetic energy ion is formed from fragmentation of a singly charged molecular ion and the high kinetic energy ion from a doubly charged molecular ion. From thermodynamic data, the minimum AP for formation of H_3^+ by each of these processes can be calculated. It is assumed that the reactions occurring are the following:

$$H_3CX + e^- \rightarrow H_3^+ + CX + 2e^- \quad (2)$$

$$H_3CX + e^- \rightarrow H_3^+ + CX^+ + 3e^- \quad . \quad (3)$$

Calculations were performed using heats of formation of the species involved compiled by Franklin, Dillard, Rosenstock, Herron, Draxl, and Field[15]. Using the heats of formation in eV per molecule, the appearance potential, assuming zero initial kinetic energy release, can be calculated.

$$AP\ (H_3^+) = \Delta H_f\ (CX) + \Delta H_f\ (H_3^+) - \Delta H_f\ (CH_3X) \quad (4)$$

In the case of the doubly charged fragmentation mechanism, the first term on the right becomes $\Delta H_f\ (CX^+)$. The heat of formation of H_3^+ was calculated from theoretical calculations of Conroy[16] on H_3^+, from which the value A = 4.73 eV was derived for the proton affinity of hydrogen. This value is higher than the experimental values of 3.0 derived from data on proton scattering in H_2 [17] and from a study of ion-molecule reactions of H_2^+ [18]. Use of A = 4.73 eV leads to a heat of formation of H_3^+ of 11.12 eV.

The calculated AP values are summarized in Table 3. To each of these is added the initial kinetic energy release, T, to obtain the minimum AP which should be observed, assuming H_3^+ to be formed in the lowest vibrational level of the $^1A_1$ ground state and CX (or CX^+) to be formed in the lowest vibrational level of the ground state. For the compounds studied, the calculated and observed AP's of the high initial kinetic energy H_3^+ component agree well with the values calculated by the doubly charged ion mechanism. In the case of C_2H_6 the observed AP of the high initial kinetic energy component of H_3^+ is, within the experimental uncertainty, equal to the value of 30.3±0.3 eV found by Olmsted, Street and Newton for the formation of high initial kinetic energy CH_3^+ ions. It is concluded that the high initial kinetic energy ions result from fragmentation of the doubly charged molecular ion.

The low initial kinetic energy component must be formed by fragmentation of a singly charged ion. The difference between the lowest calculated AP and that observed for this component, some 8 to 10 eV, suggests that the molecular ion is formed initially in a highly excited state. The experimental results suggest no disposition of this excess energy, but in all cases it is considerably higher than the C-X bond energy[19]. Several possibilities are obvious, i.e., emission of light from an excited state of CX, fragmentation of CX with release of kinetic energy, and fragmentation of CX with C being formed in an excited state. In the cases of CD_4 and CH_3Cl, the formation of D or Cl respectively in an excited state can be eliminated since in each case the energy level of the first excited state plus the C- X bond energy is higher than the excess energy available.

The wide variance in yields of H_3^+ observed from various compounds as illustrated in Fig. 12 and 13 can arise from differences in relative yields of

H_3^+ from the two independent mechanisms. In the cases examined, CD_4 and C_6H_6 show low yields of H_3^+ (at V_e = 70 V) but most of this yield is due to the low initial kinetic energy component. The higher yield of H_3^+ at V_e = 70 V from C_2H_6 and CH_3Cl respectively is due to the increased yield of the high initial kinetic energy component. Any significant correlation would require the separate consideration of these respective yields. Experimentally, other than an order of magnitude estimation, no method of measuring the separate yields was found.

The equality of AP's for the high kinetic energy ions H_3^+ and CH_3^+ from C_2H_6 suggests the doubly charged $C_2H_6^{+2}$ can fragment by at least these two paths. Olmsted, Street, and Newton[8] found the kinetic energy of the CH_3^+ satellite to be 2.45 eV, and new measurements by the metastable suppressor cutoff method yield 2.65 eV. The latter figure results in T = 5.30 eV of kinetic energy release and corresponds to a separation of charges of 2.7 Å. For separation into H_3^+ and $C_2H_3^+$, T = 4.2 eV and the separation of charges is 3.4 Å. For CH_3Cl, Olmsted, Street and Newton found the satellite of CH_3^+ to have an initial kinetic energy of 4.15 eV, corresponding to a T of 5.9 eV and a separation of charges of 2.4 Å. For separation into H_3^+ and CCl^+, T = 3.9 eV and the separation of charges is 3.7 Å. In each case the separation of charges is larger for fragmentation into $H_3^+ + CX^+$ than for fragmentation into $CH_3^+ + X^+$. This is qualitatively the result that would be expected from primitive concepts of the transition states in the two cases, H_3^+-C-X^+ and CH_3^+-X^+.

Fuchs and Taubert[13] showed that the H_2^+ ions from hydrocarbons have components of high initial kinetic energy. A metastable suppressor cutoff curve

of H_2^+ from C_2H_6 showed a component of initial kinetic energy equal to 3.7±0.1 eV. This component had an AP of 31.1±1 eV. Assuming the fragmentation process to be $C_2H_6^{+2}$ fragmenting to H_2^+ and $C_2H_4^+$, T = 4.0 eV and the separation of charges, 3.6 Å, is slightly larger than that calculated for separation into H_3^+ and $C_2H_3^+$. The suggestion implied by this data is that the same electronic state of $C_2H_6^{+2}$ can fragment by at least three independent paths. While this suggestion is consistent with the available data, it does not represent a firm conclusion.

This work was performed under the auspices of the U. S. Atomic Energy Commission.

REFERENCES

1. L. G. SMITH, Phys. Rev. 51, 263 (1937).
2. A. S. NEWTON, A. F. SCIAMANNA, and R. CLAMPITT, J. Chem. Phys. 46, 1779 (1967); 47, 4843 (1967).
3. A. S. NEWTON and A. F. SCIAMANNA, J. Chem. Phys. 50, 4868 (1969); 44, 4327 (1966).
4. "Mass Spectral Data", American Petroleum Institute Research Project 44; B. J. Zwolinski, Director, Texas A & M University, College Station, Texas.
5. C. M. LEDERER, J. M. HOLLANDER, and I. PERLMAN, Table of Isotopes, 6th edn., Wiley and Sons, Inc., New York, 1967.
6. C. E. BERRY, Phys. Rev. 78, 597 (1950).
7. R. TAUBERT, Z. Naturforsch. 19a, 484 (1964).
8. J. OLMSTED III, K. STREET, JR., and A. S. NEWTON, J. Chem. Phys. 40, 2114 (1964). Earlier references are cited in this paper.
9. R. J. KANDEL, J. Chem. Phys. 22, 1496 (1954).
10. J. OLMSTED III, "Formation of Energetic Fragment Ions by Bombardment of Organic Molecules with Slow Electrons." Dissertation, University of California, 1963; UCRL-10687, TID-4500. Available from Office of Technical Services, U. S. Department of Commerce, Washington, D. C., p. 21.
11. R. CLAMPITT and W. J. DUNNING, J. Sci. Instr. 44, 336 (1967).
12. R. FUCHS, Z. Naturforsch. 21a, 2069 (1966).
13. R. FUCHS and R. TAUBERT, Z. Naturforsch. 19a, 494 (1963).
14. A. S. NEWTON and A. F. SCIAMANNA, unpublished results (1967).
15. J. L. FRANKLIN, J. G. DILLARD, H. M. ROSENSTOCK, J. T. HERRON, K. DRAXL, and F. H. FIELD, Nat. Std. Ref. Data Ser., Nat. Bur. Std. (US), 26, U. S. Gov. Printing Office, 1969.

16. H. CONROY, J. Chem. Phys. 51, 3979 (1969).

17. J. H. SIMONS, C. M. FONTANA, E. E. MUSCHLITZ, JR., and S. R. JACKSON, J. Chem. Phys. 11, 307 (1943).

18. V. L. TAL'ROSE and E. L. FRANKEVITCH, J. Am. Chem. Soc. 80, 2344 (1958).

19. V. I. VEDENEYEV, L. V. GURVICH, V. N. KONDRAT'YEV, V. A. MEDVEDEV, and YE. L. FRANKEVITCH, Bond Energies, Ionization Potentials and Electron Affinities, Edward Arnold (Publishers) Ltd., London, 1966.

FIGURE LEGENDS

Fig. 1. Variation of peak sensitivity (peak intensity/pressure) with pressure for M/q = 2,3 and 16 from CH_4, M/q = 6 from CD_4, and M/q = 3 from C_2H_6. Conditions: I_e = 38.5 μA; V_e = 70 V; V_R = 0.0113 V_A; M/q = 2 scanned at V_A = 3000 V, 3 at 2000 V, 6 at 2000 V and 16 at 2840 V.

Fig. 2. Ion accelerating voltage discrimination curves of H_3^+ ions from CH_4 and C_2H_6, and D_3^+ ions from CD_4.

Fig. 3. Repeller cutoff curves of H_3^+ ions from CH_4, and D_3^+ ions from CD_4. Conditions: V_e = 70 V; V_A = 3000 V; repellers equal; magnetic scan.

Fig. 4. Metastable suppressor cutoff curves of $^{22}Ne^+$ ions and D_3^+ ions from a mixture of ^{22}Ne and CD_4. Conditions: V_A = 2000 V; repellers equal at 0.008 V_A; 1.000 V_{mss} = 2097 V; V_e = 81 V; magnetic scan.

Fig. 5. Repeller cutoff curves of H_3^+ ions from C_2H_6 and H_3^+ ions from CH_3Cl. Conditions: V_e = 90 V; V_A = 3000 V; repellers equal; magnetic scan.

Fig. 6. Metastable suppressor cutoff curves of He^+ ions and H_3^+ ions from a mixture of 1% He gas in C_2H_6 at corrected ionizing electron energies of 83 eV and 33 eV. Conditions: V_A = 2000 V; repellers equal at 0.01 V_A; 1.000 V_{mss} = 2097 V; magnetic scan.

Fig. 7. Metastable suppressor cutoff curves of He^+ ions and H_3^+ ions from a mixture of 1% He gas in CH_3Cl at corrected ionizing electron energies of 83 eV and 32.3 eV. Conditions: V_A = 2000 V; repellers equal at 0.01 V_A; 1.000 V_{mss} = 2097 V; magnetic scan.

Fig. 8. Ionization efficiency curves for the formation of H_3^+ from CH_4, and D_3^+ from CD_4. Conditions: V_A = 3000 V; V_R = 0.0065 V_A; inlet pressure = 100 μm Voltage scale corrected by appearance potentials of $He^+(CH_4)$ and $^{22}Ne^+(CD_4)$.

Fig. 9. Ionization efficiency curves for formation of D_3^+ ions from CD_4. Variation of curves with fraction of metastable suppressor voltage applied at collector. Conditions: V_A = 2000 V; repellers equal at 0.008 V_A; 1.000 V_{mss} = 2097 V; magnetic scan. Electron energy scale corrected to first appearance of D_3^+ at 25.5 eV with f_{mss} = 0.970.

Fig. 10. Ionization efficiency curves for formation of He^+ and H_3^+ ions from a mixture of 1% He in C_2H_6. Variation of H_3^+ curves with fraction of metastable suppressor voltage applied at collector. Conditions: V_A = 2000 V; repellers equal at 0.01 V_A; 1.000 V_{mss} = 2097 V; magnetic scan. Electron energy scale corrected to first appearance of He^+ at 24.6 eV with f_{mss} = 0.980.

Fig. 11. Ionization efficiency curves for formation of He^+ and H_3^+ from a mixture of 1% He in CH_3Cl. Variation of H_3^+ curves with fraction of metastable suppressor voltage applied at collector. Conditions: V_A = 2000 V; repellers equal at 0.01 V_A; 1.000 V_{mss} = 2097 V; magnetic scan. Electron energy scale corrected to first appearance of He^+ at 24.6 eV.

Fig. 12. Variation of yields of H_2^+ and H_3^+ in the n-alkanes and of H_3^+ in the 1-alkenes with carbon number.

Fig. 13. Variation of yields of H_2^+, H_3^+, and H_2X^+ in the methyl halides.

Table 1. Observed Yields of H_3^+ Ion from Various Compounds.

Compounds	H_3^+/H_2^+ [a]	Pattern H_3^+ [b]	Pattern H_2X^+ [e]
Alkanes			
CH_4	0.0088[c]	0.0038	
CD_4	0.0086[d]	-	
C_2H_6	0.143	0.064	
C_3H_8	0.146	0.025	
n-C_4H_{10}	0.065	0.0076	
i-C_4H_{10}	0.067	0.0072	
neo-C_5H_{12}	0.037	0.0026	
i-C_5H_{12}	0.033	0.0033	
n-C_5H_{12}	0.038	0.0041	
n-C_6H_{14}	0.029	0.0021	
n-C_7H_{16}	0.017	0.0012	
n-C_8H_{18}	0.013	0.0008	
2,2,4-trimethyl-pentane	0.016	0.0012	
Alkenes, polyolefins, and aromatics			
C_2H_4	0.0097[c]	0.0032	
C_3H_4(methyl acetylene)	0.029	0.0049	
C_3H_6	0.076	0.021	
1,2-C_4H_6	0.025	0.0046	
1,3-C_4H_6	0.018	0.0033	
1-C_4H_8	0.030	0.0055	
2-C_4H_8(cis)	0.036	0.0079	

(continued)

Table 1. Continued.

Compounds	H_3^+/H_2^+ [a]	Pattern H_3^+ [b]	Pattern H_2X^+ [c]
Alkenes, polyolefins, and aromatics, continued			
$2\text{-}C_4H_8$(trans)	0.036	0.0075	
$i\text{-}C_4H_8$	0.030	0.0061	
2-methylbutene-2	0.025	0.0036	
hexene-1	0.017	0.0019	
2,2,4-trimethyl-pentene-1	0.013	0.0014	
benzene	0.037	0.0025	
Misc. compounds			
CH_3F	0.017	0.0051	0.0024 (H_2F^+)
CH_3Cl	0.215	0.043	0.026 (H_2Cl^+)
CH_3Br	0.200	0.024	0.031 (H_2Br^+)
CH_3I	0.016	0.0014	0.015 (H_2I^+)
CH_3OH	0.053	0.028	0.11 (H_3O^+)
C_2H_5OH	0.076	0.025	1.3 (H_3O^+)
C_2H_5Cl	0.075	0.016	0.12 (H_2Cl^+)
CH_3CF_3	0.024	0.0054	0.038 (H_2F^+)

[a] The H_3^+ peak scanned at 2000 V ion accelerating voltage, the H_2^+ peak at 3000 V; each at 70 V nominal ionizing voltage, normal repellers of $\sim$0.01 V_A, 0.5 mm collector slit.

[b] Patterns are expressed as the percent the H_3^+ peak intensity contributes to the total peak intensity.

(continued)

Table 1. Continued.

[c] Corrected for contribution of HD^+ from the H_2^+ peak.

[d] D_3^+/D_2^+ ratio.

[e] H_2X^+ peak intensity as % of total peak intensity.

Table 2. Energetics of Formation of H_3^+ from Various Compounds

Compound	A.P. (H_3^+) (eV)	Standard	Initial K.E. H_3^+ (eV)	Relative Yield (Est.) V_e = 70 V	Method[a]	T[b]
CH_4	25.0±1[c]	He^+	⩽ 0.7	> 90%	NR	⩽ 0.85
	(25.3±1)[d]		4.9±0.2	< 10%	NR	6.0±0.3
CD_4	25.5±0.5	$^{22}Ne^+$	⩽ 0.1	> 90%	mss	⩽ 0.14
	35.5±2[e]		4.0±0.2	< 10%	mss	5.7±0.3
			⩽ 0.5	> 90%	NR	
			3.9±0.2	< 10%	NR	
C_2H_6	24.6±0.5	He^+	⩽ 0.1	< 10%	mss	⩽ 0.11
	30.0±1[e]	He^+	3.8±0.1	> 90%	mss	4.2±0.1
			4.3±0.2		NR	
			4.1±0.2		S	
CH_3Cl	25.5±0.5	He^+	⩽ 0.2	< 10%	mss	⩽ 0.21
	29.9±1[e]	He^+	3.7±0.1	> 90%	mss	3.9±0.1
			4.1±0.2		NR	
C_6H_6			⩽ 0.2	> 80%	mss	
			3.8±0.3	< 20%	mss	
C_4H_{10}	26 ±2[c]	He^+				
C_2H_4	22.7±1[c]	He^+				

[a] NR - negative repeller method, mss - metastable suppressor cutoff method, S - satellite method.

[b] Total fragmentation energy, T, assuming fragmentation to be $H_3CX^+ \rightarrow H_3^+ + CX$.

[c] Weak onset over background of HD^+ or lower state of low transition probability.

[d] From reference 1.

[e] A.P. of high initial kinetic energy state.

Table 3. Comparison of Calculated and Observed Appearance Potentials for the Formation of D_3^+ from CD_4 and H_3^+ from C_2H_6 and CH_3Cl.

Products	CD_4[a]		C_2H_6		CH_3Cl	
	$D_3^+ + CD$	$D_3^+ + CD^+$	$H_3^+ + C_2H_3$	$H_3^+ + C_2H_3^+$	$H_3^+ + CCl$	$H_3^+ + CCl^+$
$-\Delta H_f(CH_3X)$[b]	0.78	0.78	0.88	0.88	0.84	0.84
$\Delta H_f(CX)$	6.17		2.82		5.29	
$\Delta H_f(CX^+)$		17.30		11.67[c]		13.70[d]
$\Delta H_f(H_3^+)$[e]	11.12	11.12	11.12	11.12	11.12	11.12
Σ = Min A.P. at T=0	18.07	29.20	14.82	23.67	17.25	25.66
T	$\leqslant$ 0.2	5.7	$\leqslant$ 0.1	4.2	$\leqslant$ 0.2	3.9
Calc A.P.	$\leqslant$ 18.3	34.9	$\leqslant$ 14.9	27.9	$\leqslant$ 17.4	29.6
Obs A.P.	25.5±0.5	35.5±2	25.0±0.5	30.0±0.5	25.5±0.5	29.9 ±1
ΔA.P. (Obs-Calc)	7.2±0.5	0.6±2	10.1±0.5	2.1±0.5	8.1±0.5	0.3±1

[a] Assuming heats of formation of deuterated species equal to those given in Ref. 15 for protonated species.

[b] All heats of formation expressed in eV/molecule.

[c] Assuming $\Delta H_f(C_2H_3^+)$ = 269 Kcal/mole. (Ref. 15).

[d] Assuming $\Delta H_f(CCl^+)$ = 316 Kcal/mole. Listed values range from 316 to 420 Kcal/mole. (Ref. 15).

[e] Calculated assuming the proton affinity of H_2 to be 4.73 eV.

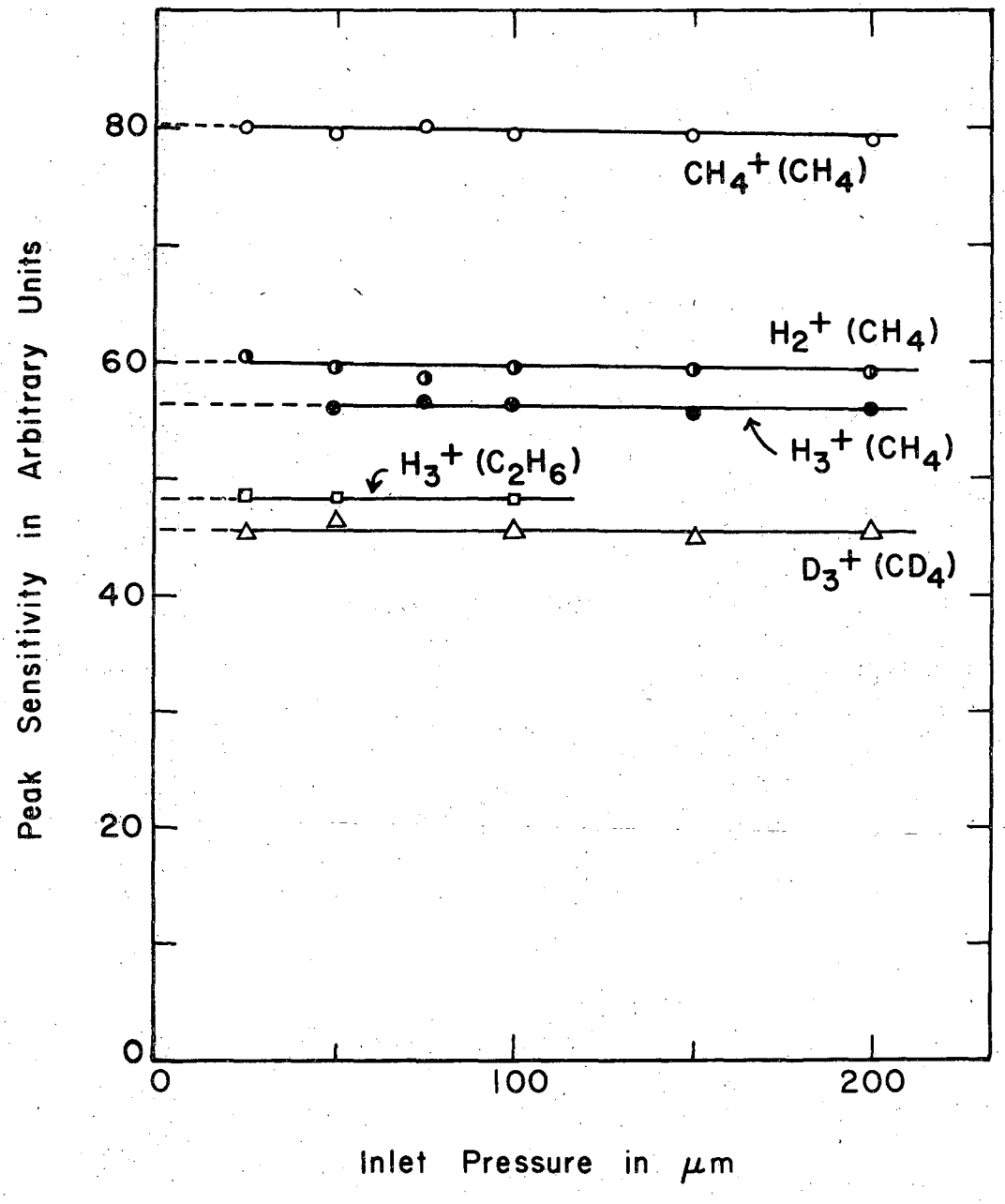
80
60
40
20
0
0
100
200
Peak Sensitivity in Arbitrary Units
Inlet Pressure in μm
CH4+ (CH4)
H2+ (CH4)
H3+ (CH4)
H3+ (C2H6)
D3+ (CD4)
XBL 706-1090

Fig. 1

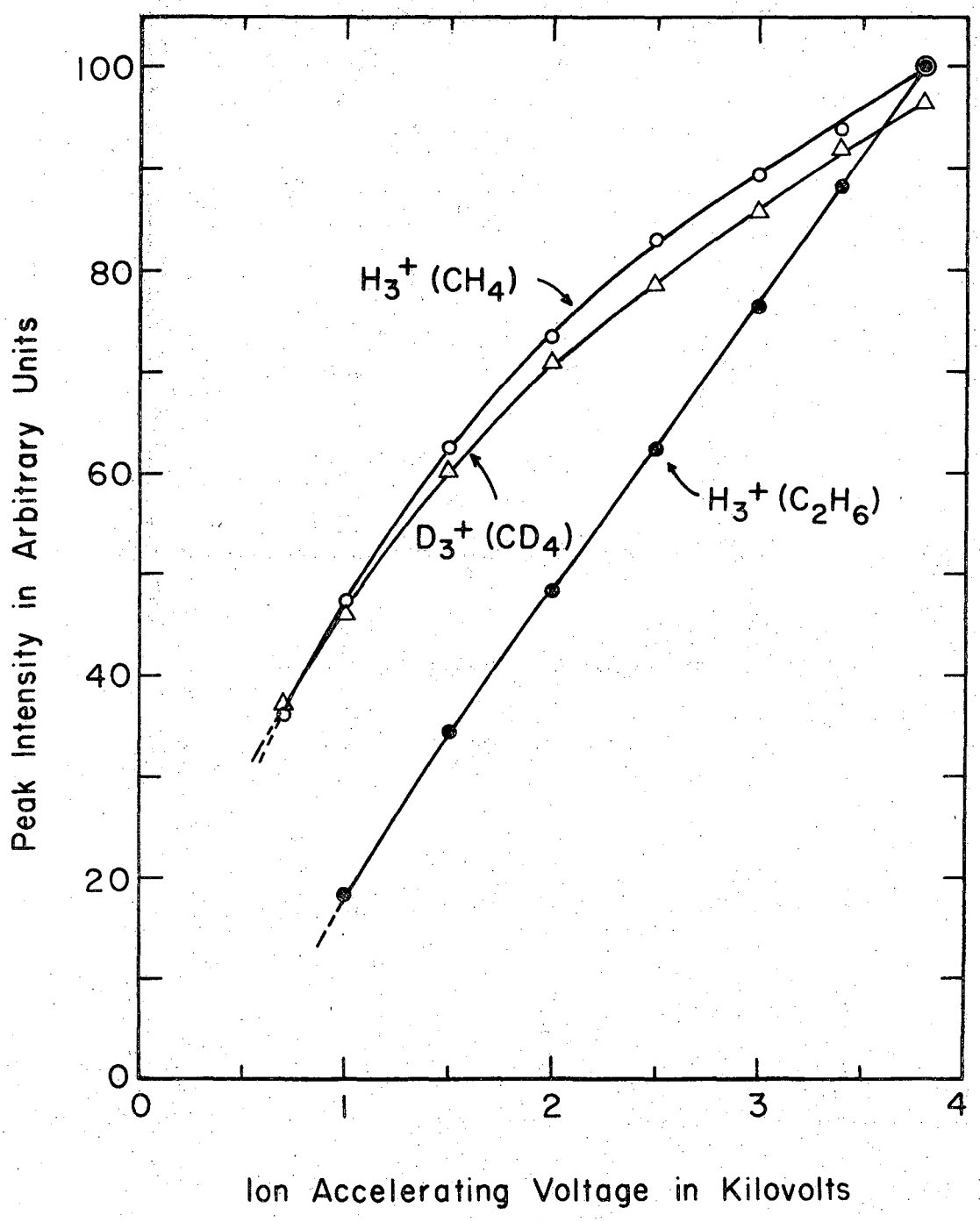

XBL 706-1091

Fig. 2

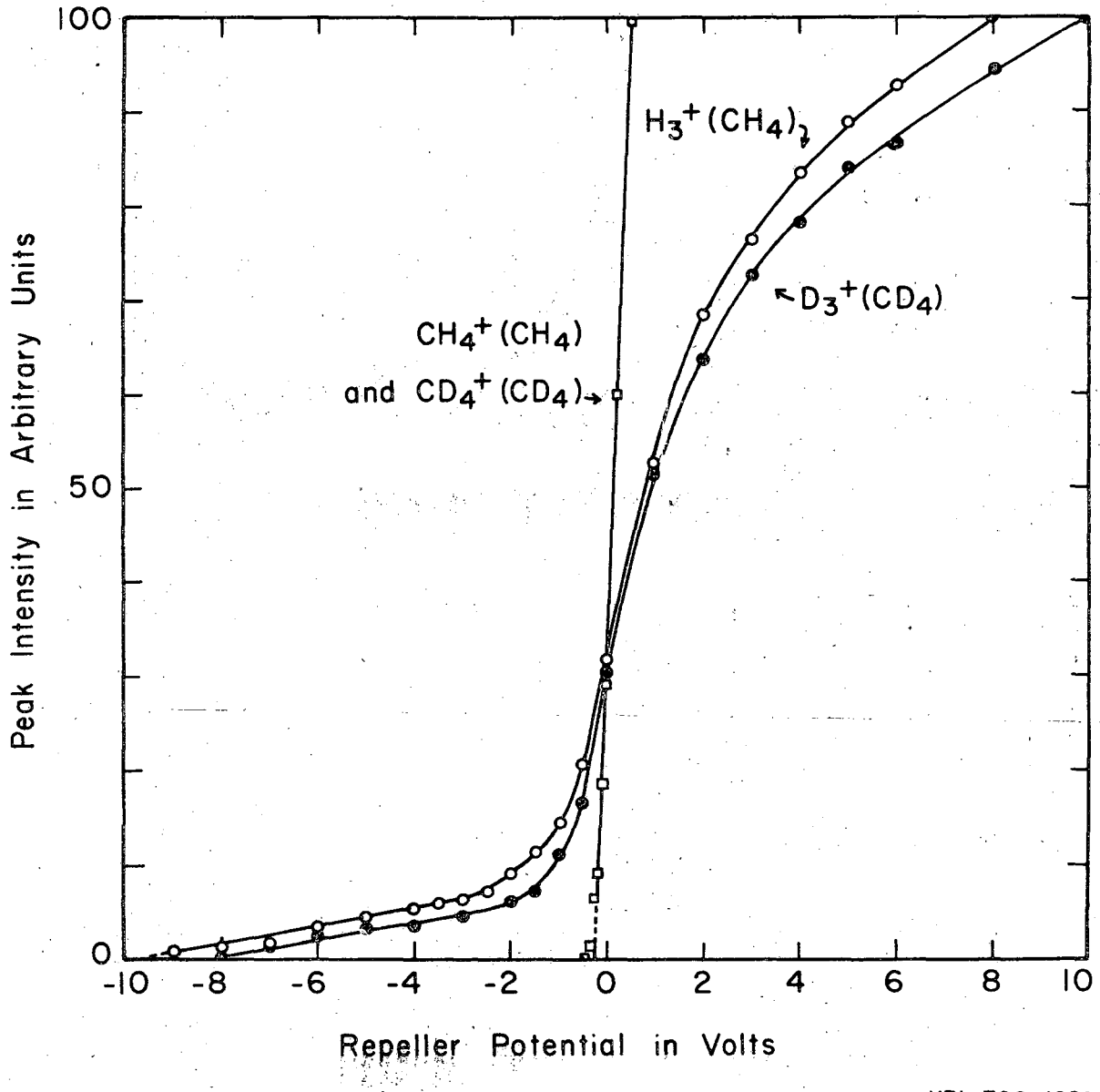
100
50
0
-10
-8
-6
-4
-2
0
2
4
6
8
10
Peak Intensity in Arbitrary Units
Repeller Potential in Volts
$H_3^+(CH_4)_2$
$D_3^+(CD_4)$
$CH_4^+(CH_4)$
and $CD_4^+(CD_4)$
XBL 706-1093

Fig. 3

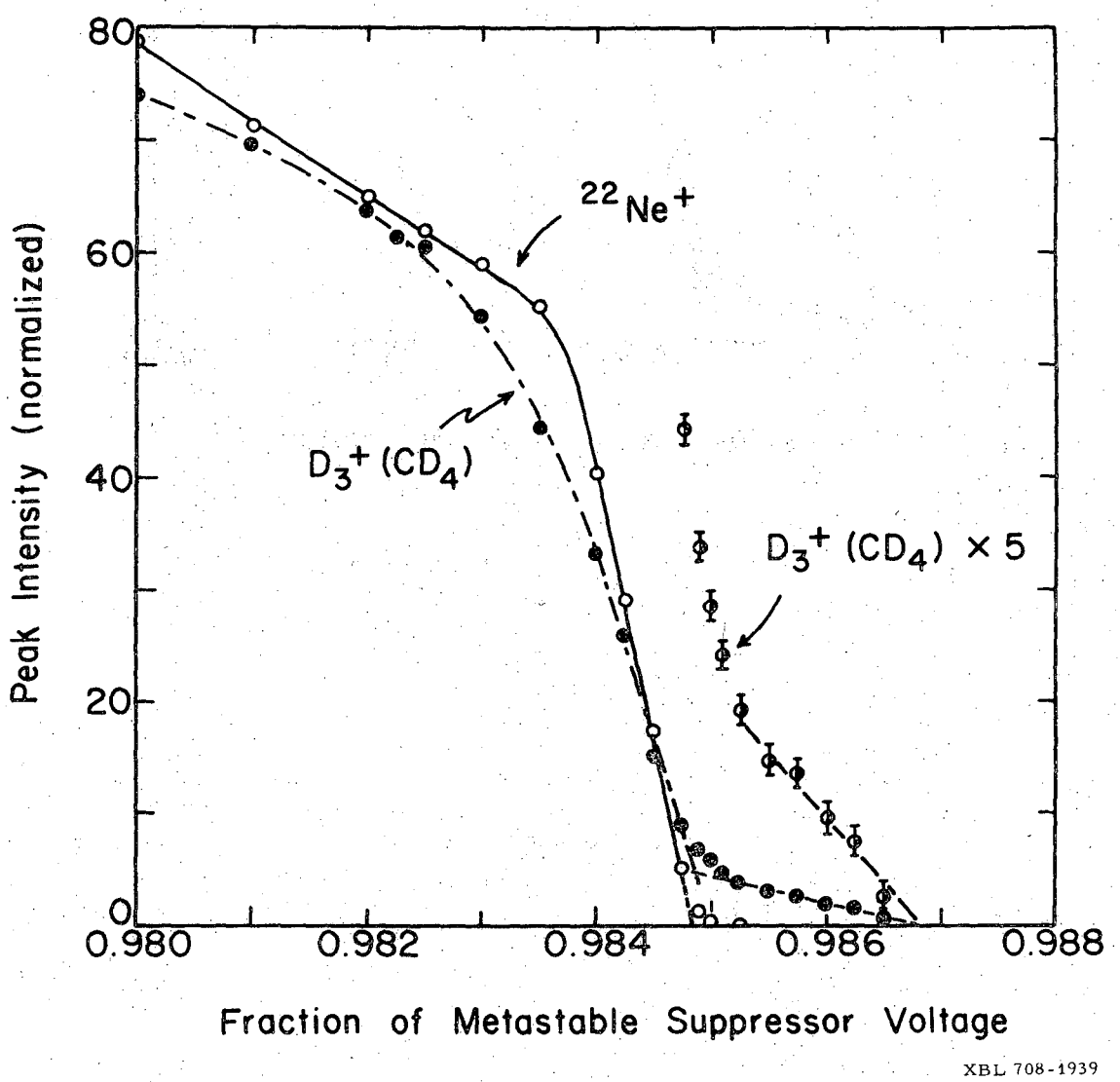
80
60
40
20
0
Peak Intensity (normalized)
$^{22}Ne^+$
$D_3^+ (CD_4)$
$D_3^+ (CD_4) \times 5$
0.980
0.982
0.984
0.986
0.988
Fraction of Metastable Suppressor Voltage
XBL 708-1939

Fig. 4

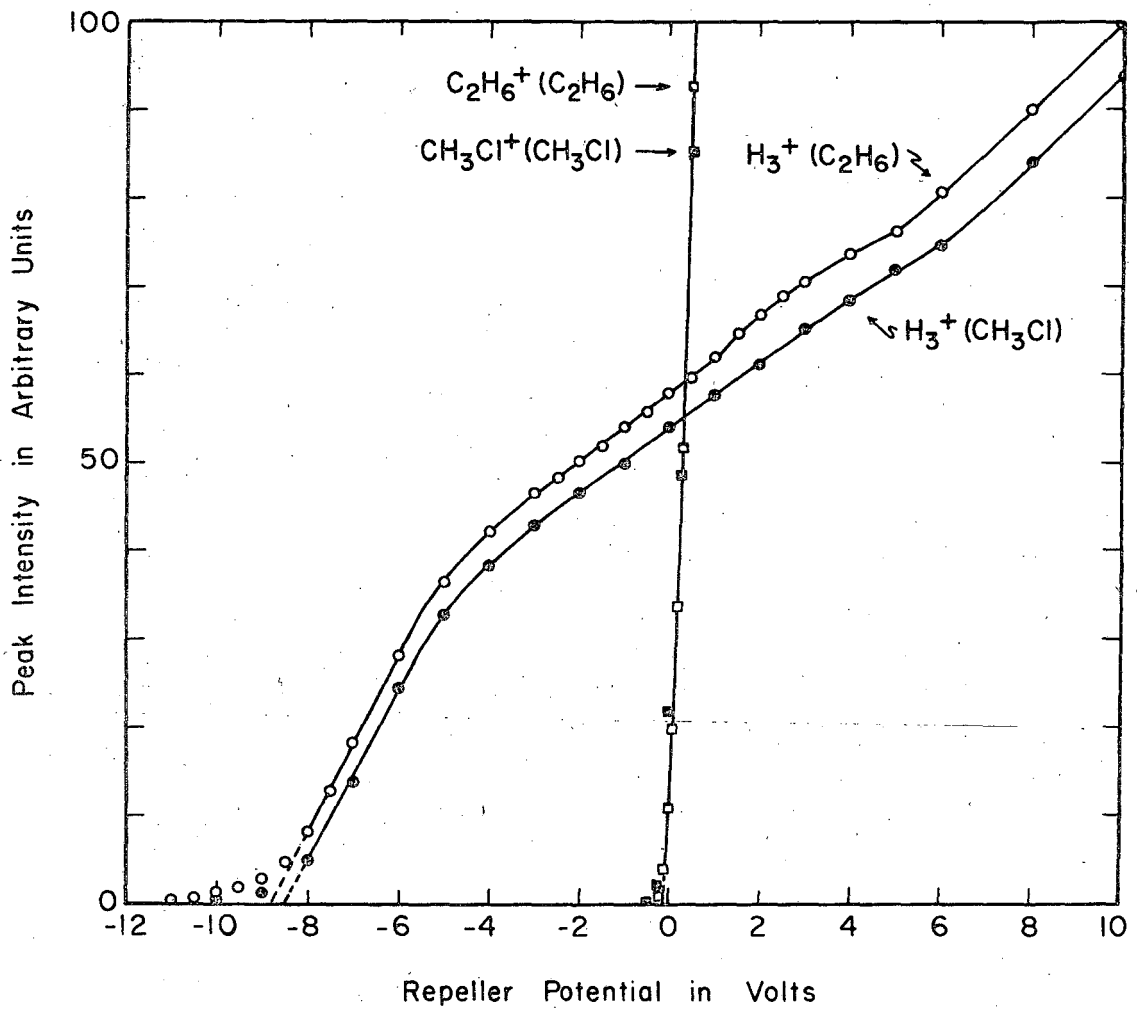
100
50
0
-12
-10
-8
-6
-4
-2
0
2
4
6
8
10
Peak Intensity in Arbitrary Units
Repeller Potential in Volts
$C_2H_6^+(C_2H_6)$
$CH_3Cl^+(CH_3Cl)$
$H_3^+(C_2H_6)$
$H_3^+(CH_3Cl)$
XBL 706-1095

Fig. 5

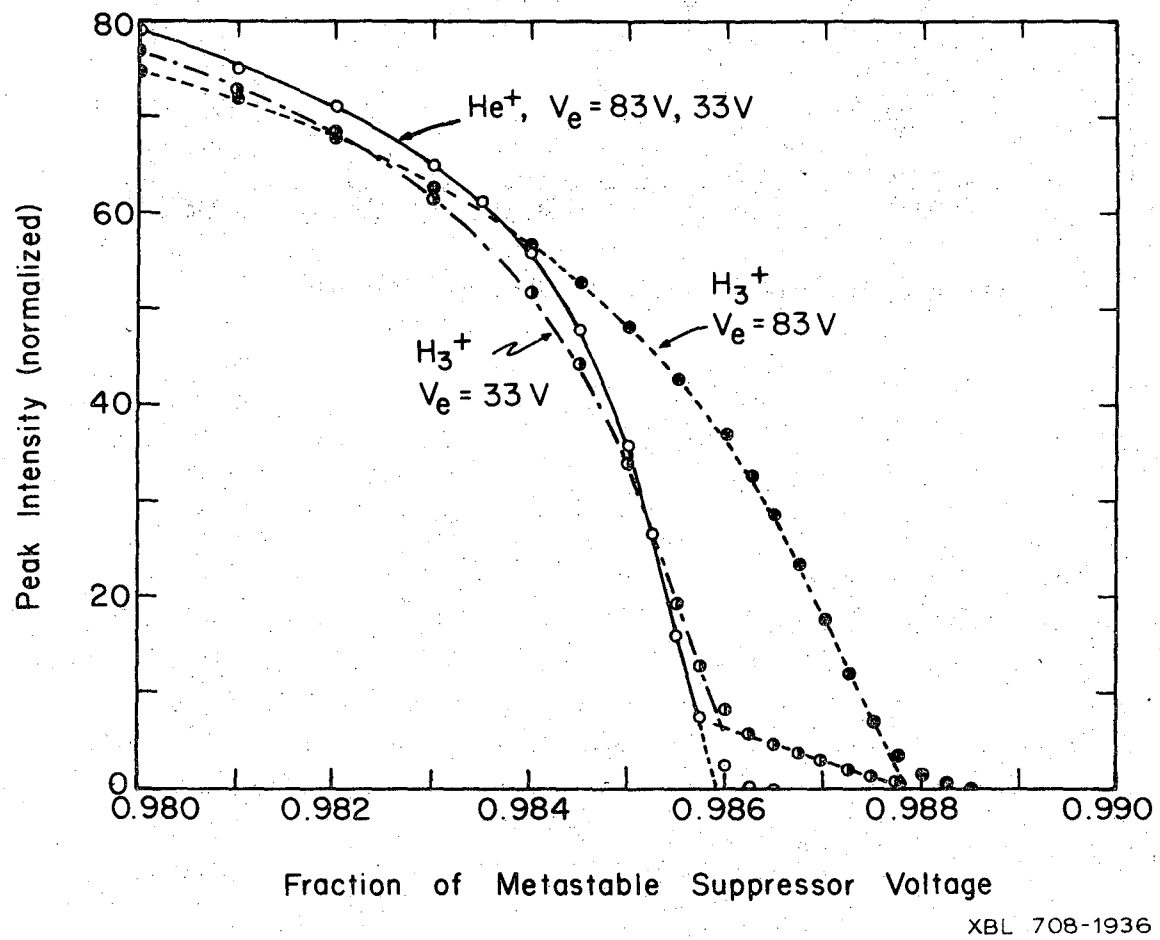
80
60
40
20
0
Peak Intensity (normalized)
He+, Ve = 83V, 33V
H3+
Ve = 83 V
H3+
Ve = 33 V
0.980
0.982
0.984
0.986
0.988
0.990
Fraction of Metastable Suppressor Voltage
XBL 708-1936

Fig. 6

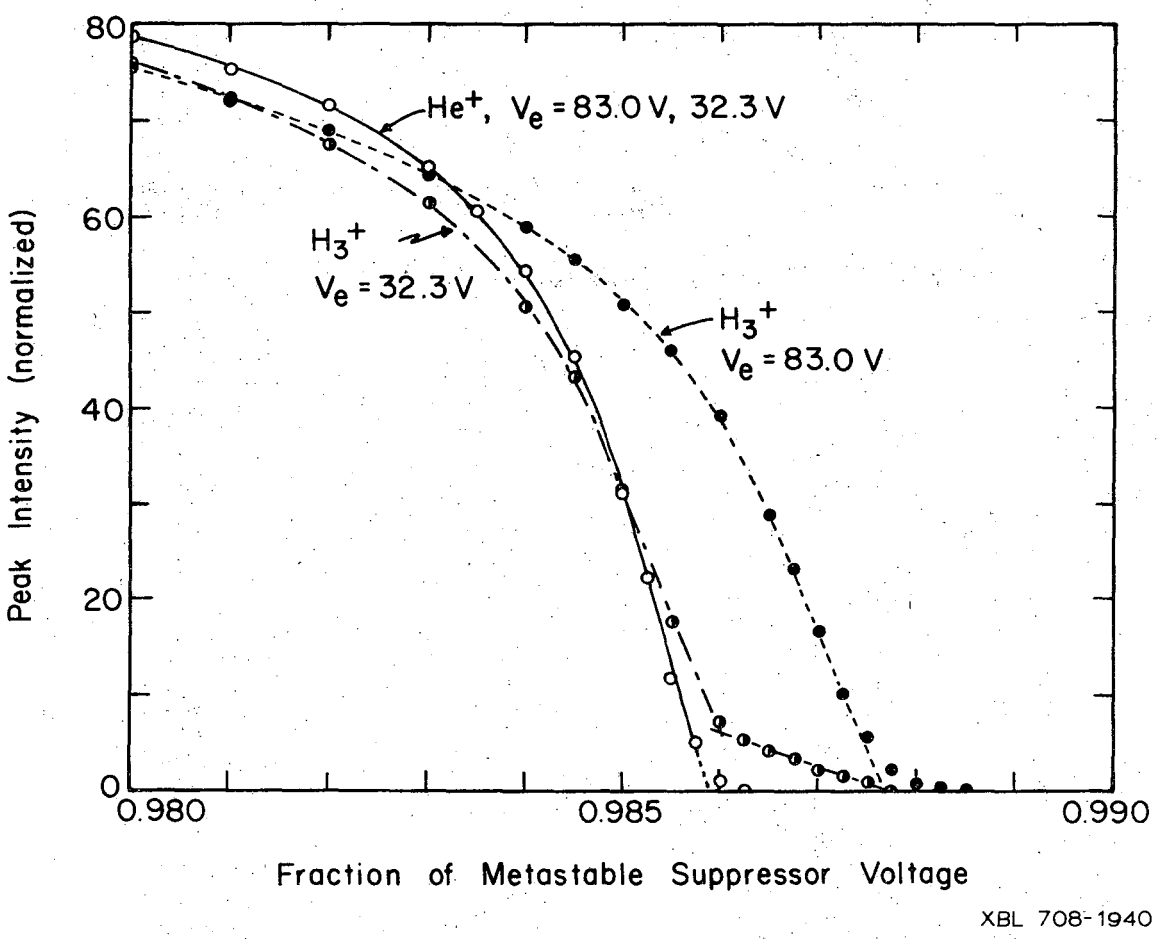
80
60
40
20
0
Peak Intensity (normalized)
0.980
0.985
0.990
Fraction of Metastable Suppressor Voltage
He+, Ve = 83.0 V, 32.3 V
H3+
Ve = 32.3 V
H3+
Ve = 83.0 V
XBL 708-1940

Fig. 7

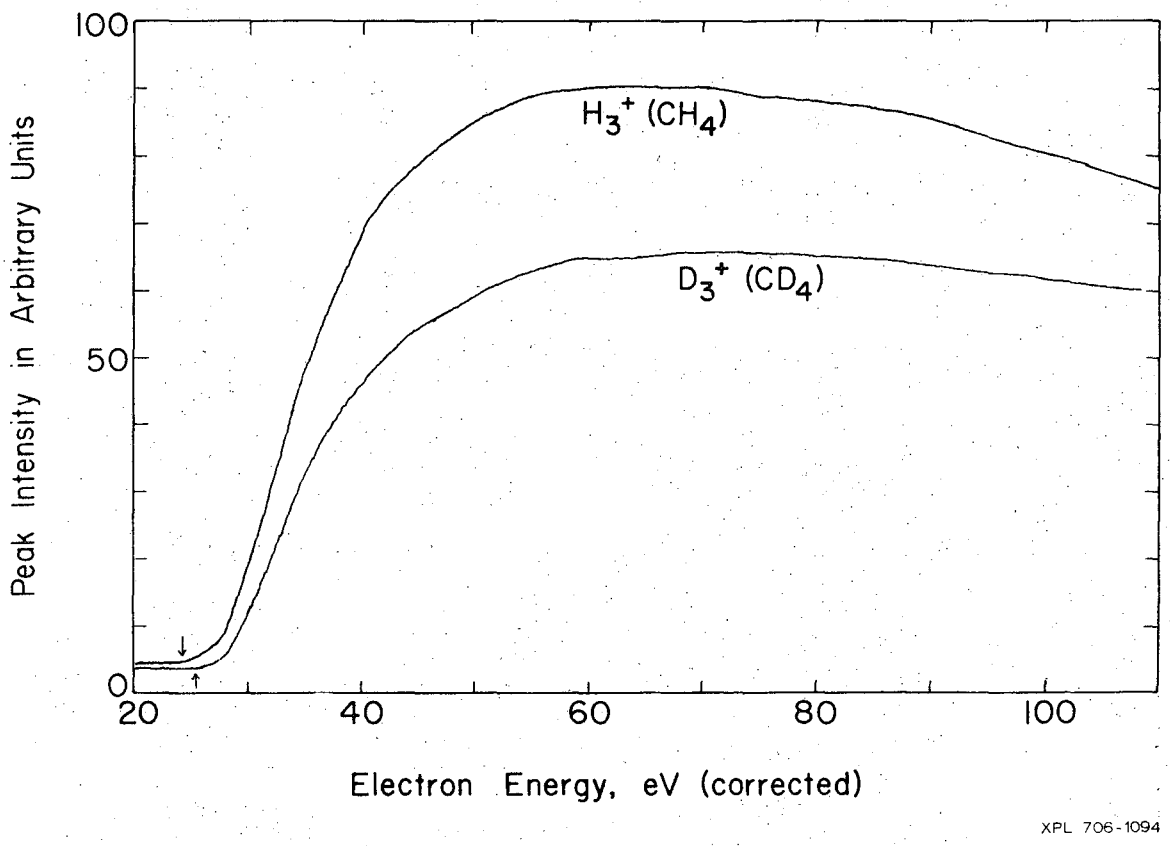
100
50
0
20
40
60
80
100
Peak Intensity in Arbitrary Units
Electron Energy, eV (corrected)
H_3^+ (CH_4)
D_3^+ (CD_4)
XPL 706-1094

Fig. 8

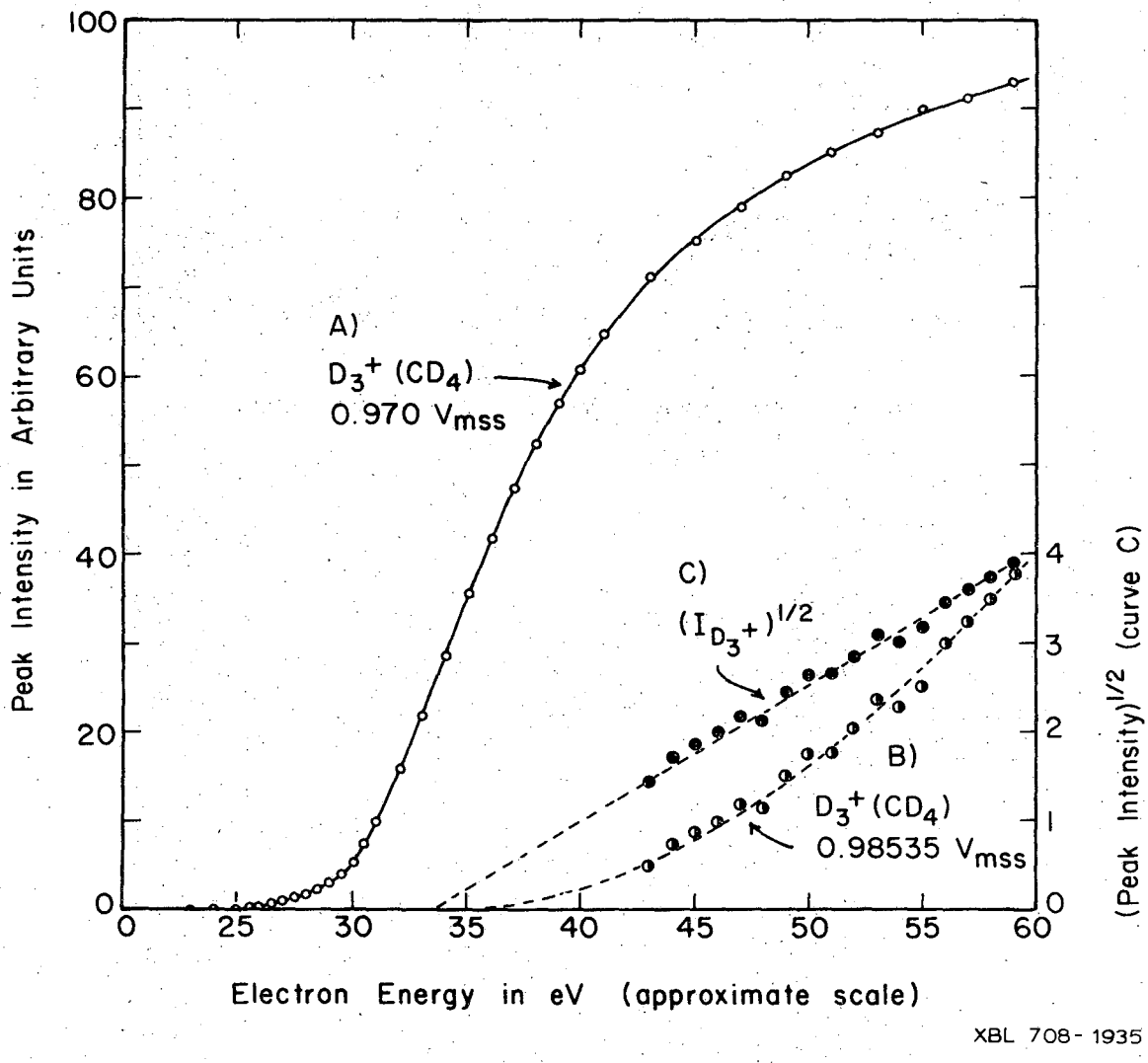
100
80
60
40
20
0
Peak Intensity in Arbitrary Units
A)
D_3^+ (CD_4)
0.970 V_{mss}
C)
$(I_{D_3^+})^{1/2}$
B)
D_3^+ (CD_4)
0.98535 V_{mss}
0
25
30
35
40
45
50
55
60
Electron Energy in eV (approximate scale)
4
3
2
1
0
$(Peak\ Intensity)^{1/2}$ (curve C)
XBL 708-1935

Fig. 9

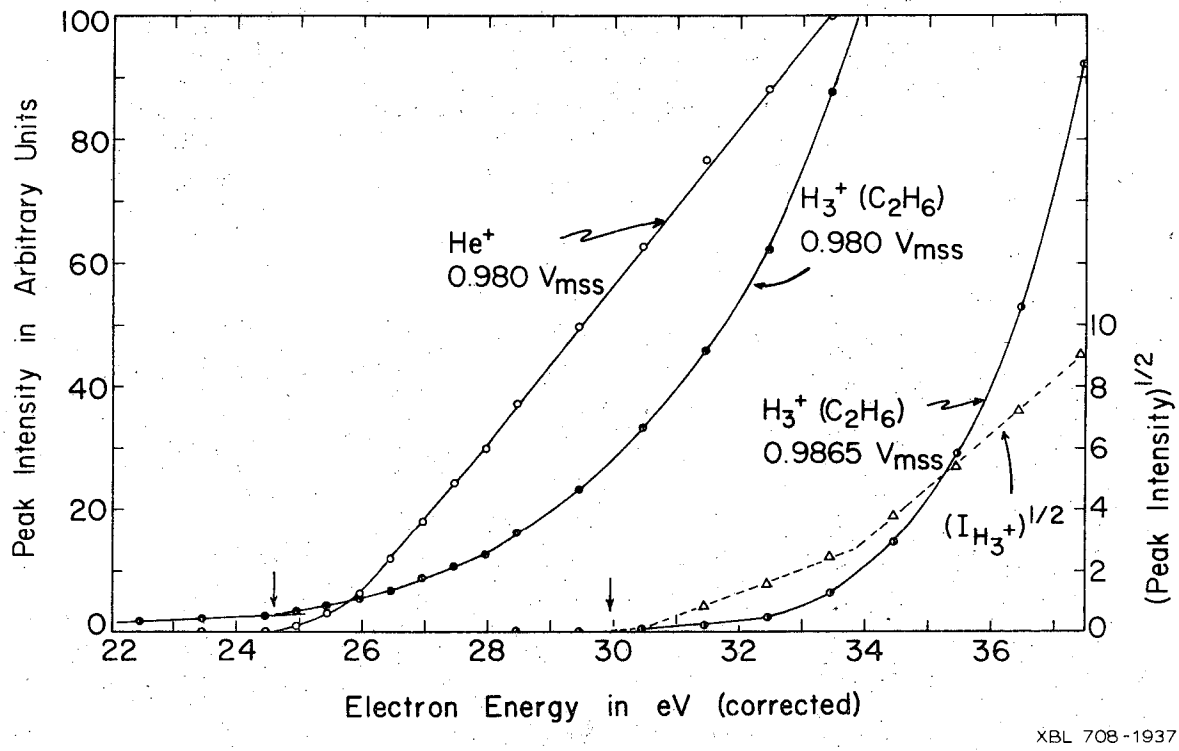
Peak Intensity in Arbitrary Units
(Peak Intensity)$^{1/2}$
Electron Energy in eV (corrected)
He$^+$
0.980 V_{mss}
H_3^+ (C_2H_6)
0.980 V_{mss}
H_3^+ (C_2H_6)
0.9865 V_{mss}
$(I_{H_3^+})^{1/2}$
XBL 708-1937

Fig. 10

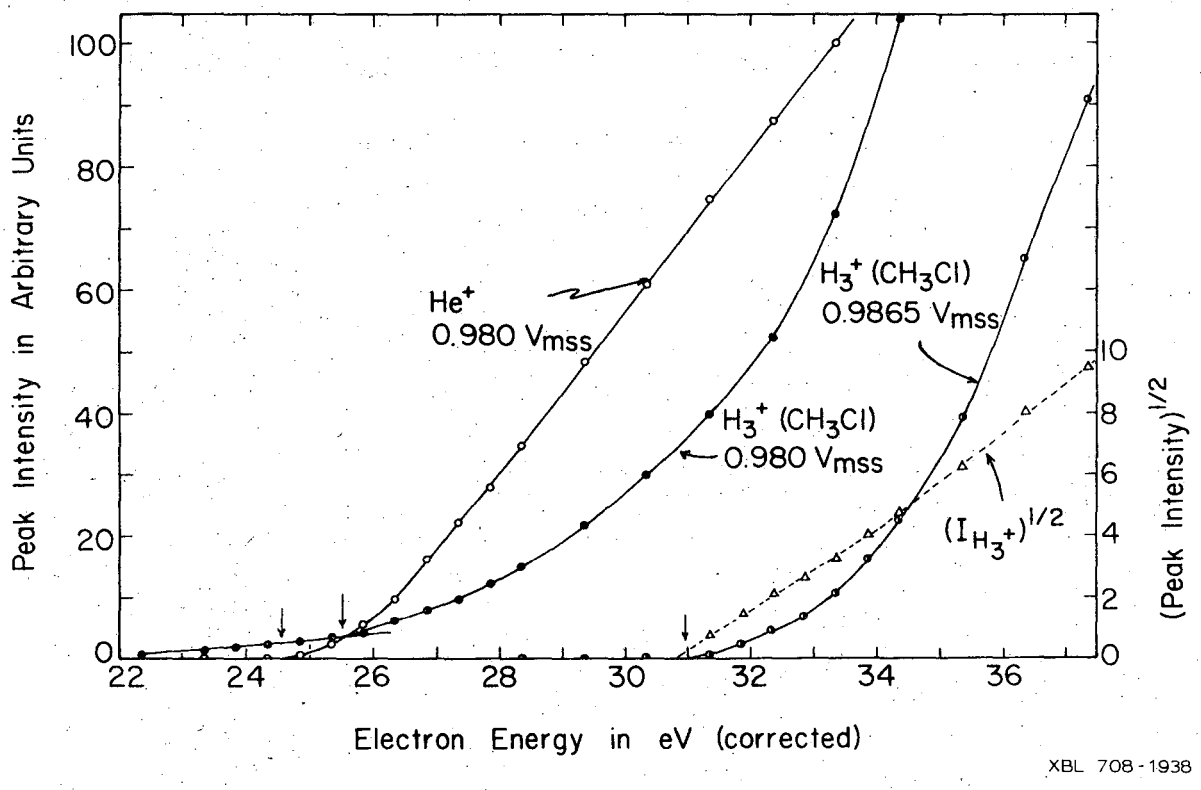
Peak Intensity in Arbitrary Units
(Peak Intensity)$^{1/2}$
Electron Energy in eV (corrected)
He^+
0.980 V_{mss}
H_3^+ (CH_3Cl)
0.9865 V_{mss}
H_3^+ (CH_3Cl)
0.980 V_{mss}
$(I_{H_3^+})^{1/2}$
XBL 708-1938

Fig. 11

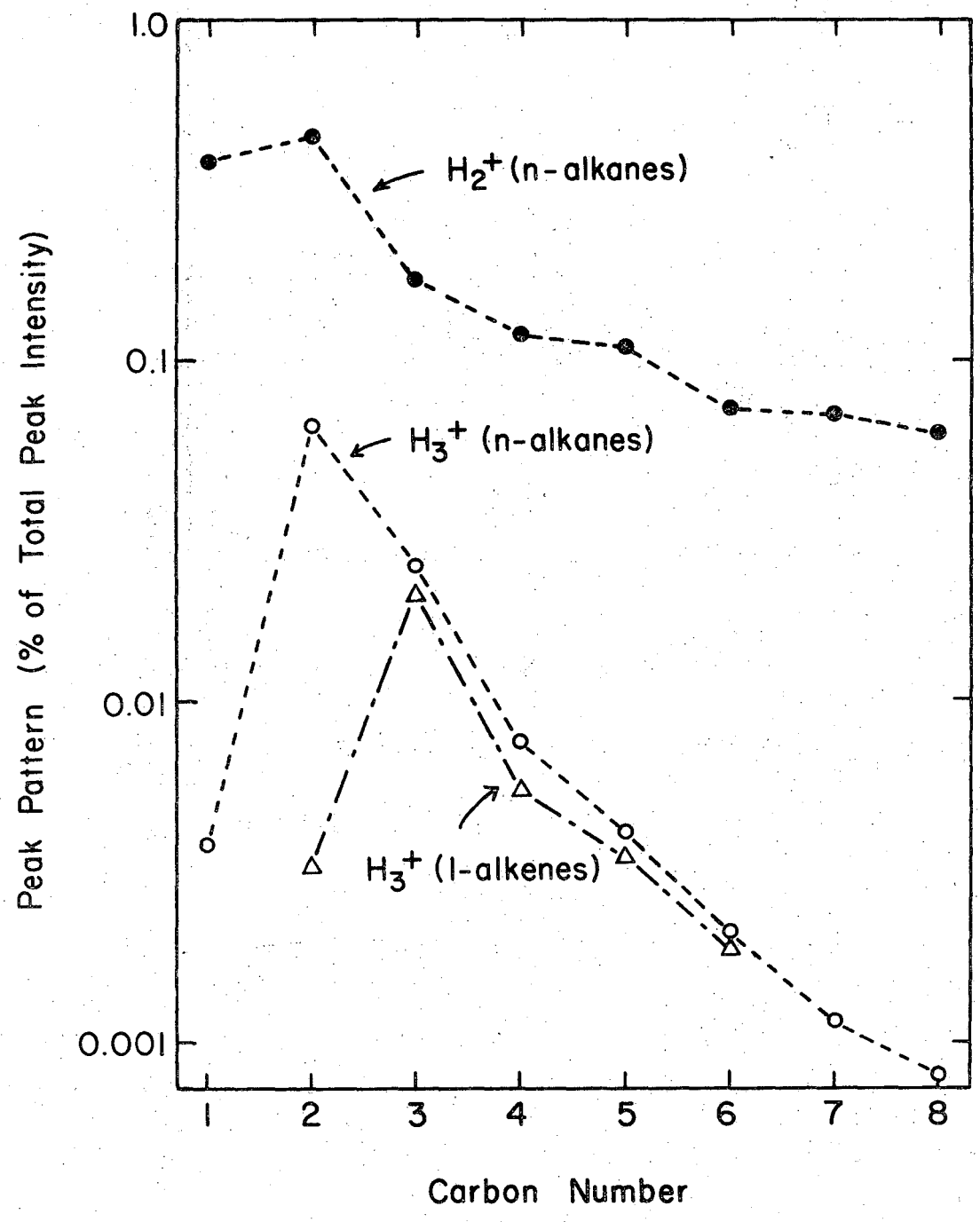

XBL 706-1089

Fig. 12

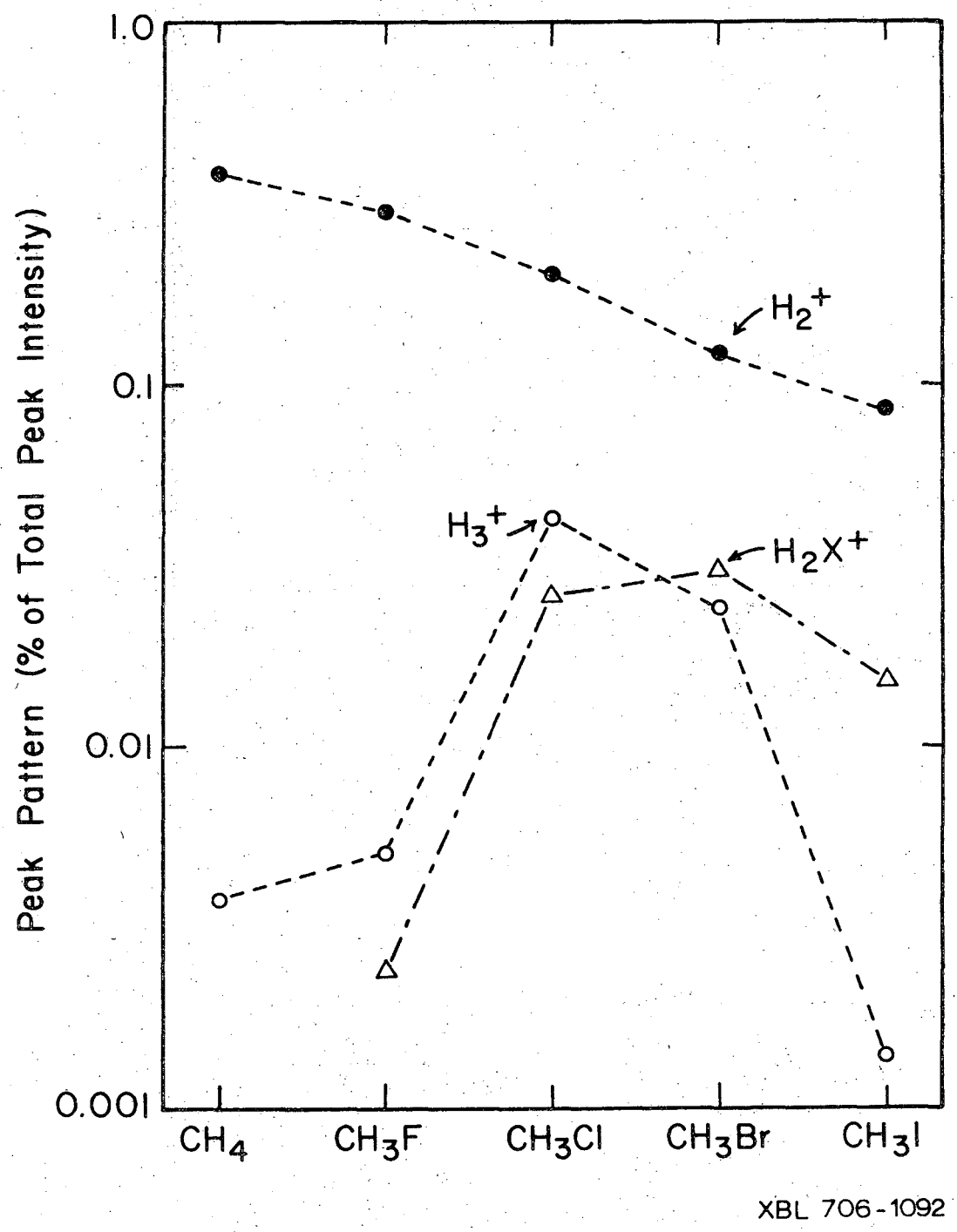
1.0
0.1
0.01
0.001
Peak Pattern (% of Total Peak Intensity)
H_2^+
H_3^+
H_2X^+
CH_4
CH_3F
CH_3Cl
CH_3Br
CH_3I
XBL 706-1092

Fig. 13

LEGAL NOTICE

This report was prepared as an account of Government sponsored work. Neither the United States, nor the Commission, nor any person acting on behalf of the Commission:

A. Makes any warranty or representation, expressed or implied, with respect to the accuracy, completeness, or usefulness of the information contained in this report, or that the use of any information, apparatus, method, or process disclosed in this report may not infringe privately owned rights; or

B. Assumes any liabilities with respect to the use of, or for damages resulting from the use of any information, apparatus, method, or process disclosed in this report.

As used in the above, "person acting on behalf of the Commission" includes any employee or contractor of the Commission, or employee of such contractor, to the extent that such employee or contractor of the Commission, or employee of such contractor prepares, disseminates, or provides access to, any information pursuant to his employment or contract with the Commission, or his employment with such contractor.

TECHNICAL INFORMATION DIVISION
LAWRENCE RADIATION LABORATORY
UNIVERSITY OF CALIFORNIA
BERKELEY, CALIFORNIA 94720